MAUSAM, **76**, 4 (October 2025), 1207-1222

MAUSAM

DOI: https://doi.org/10.54302/mausam.v76i4.7093
Homepage: https://mausamjournal.imd.gov.in/index.php/MAUSAM

UDC No. 551.553.21:551.509.313.43

Potential impacts of mesoscale assimilation of non-conventional data on rainfall characteristics of monsoon depressions during Southwest monsoon

KRISHNA K OSURI[1*], JHARNA BORAH[1#], KOUSHIK K[1@], Y. SRINIVAS NEKKALI[1$], RAGHU NADIMPALLI[2€] and VIJAY KUMAR SONI[2¥]

[1]*Department of Earth and Atmospheric Sciences, NIT Rourkela (#jharnaborah7086@gmail.com, @kkoushikh97@gmail.com, $yernisrinivasnekkali@gmail.com)*

[2]*India Meteorological Department, New Delhi (€raghu.met2012@gmail.com, ¥soni_vk@yahoo.com*)

(*Received 06 May 2024, Accepted 15 September 2025*)

***Corresponding author's email: osurikishore@gmail.com**

सार – यह अध्ययन उन्नत अनुसंधान मौसम अनुसंधान और पूर्वानुमान (ARW) मॉडल की प्रारंभिक स्थितियों को बेहतर बनाने में उपग्रह विकिरणों के आत्मसात से संबंधित है और मॉनसून अवसाद (MDs) से जुड़े वर्षा और अन्य मौसम संबंधी विशेषताओं के सिमुलेशन पर इसका प्रभाव है। अध्ययन के लिए 2015-2018 के दौरान होने वाले आठ एमडी को ध्यान में रखा गया है। दो संख्यात्मक प्रयोगों का एक सेट: CNTL, बिना किसी डेटा आत्मसात के, और SAT, जहां उपग्रह विकिरणों को मॉडल की प्रारंभिक स्थिति में आत्मसात किया जाता है, प्रत्येक MD मामले के लिए आयोजित किया जाता है। इस अध्ययन में, NOAA 15, NOAA 18, NOAA 19, EOS 2, METOP 1 और METOP 2 पर साउंडिंग इंस्ट्रूमेंट्स एडवांस्ड माइक्रोवेव साउंडिंग यूनिट (AMSU), माइक्रोवेव साउंडिंग यूनिट (MHS), और एटमॉस्फेरिक इंफ्रारेड साउंडर (AIRS) से सैटेलाइट रेडिएशन डेटा का इस्तेमाल किया गया है। राष्ट्रीय मौसम विज्ञान केंद्र (एनएमसी) पद्धति का उपयोग करके जून से अगस्त 2017 के लिए गणना की गई क्षेत्र-विशिष्ट पृष्ठभूमि त्रुटि सांख्यिकी का उपयोग करके यह समावेशन किया गया है।

समावेशन के बाद एमडी के ट्रैक में 12 घंटे से 42 घंटे तक सुधार देखा गया है, जिसमें एसएटी रन के लिए न्यूनतम ट्रैक त्रुटि 320 किमी है, जबकि सीएनटीएल रन के लिए यह 400 किमी है। मुख्यतः ऊपरी क्षोभमंडलीय स्तरों पर पवनों का अनुकरण, आत्मसातीकरण के काफी बाद किया गया, जबकि निचले स्तर की पवनों के लिए, आत्मसातीकरण लंबी दूरी के पूर्वानुमान (>24 घंटे) के लिए विश्वसनीय हैं। TRMM वर्षा और भारतीय मौसम विज्ञान विभाग (IMD) स्टेशन के प्रेक्षणों की तुलना में, CNTL रन की तुलना में, आत्मसातीकरण रन, वर्षण की तीव्रता और स्थानिक प्रसार, दोनों को बेहतर ढंग से दर्शाते हैं। इसके अलावा, SAT रन में अनुकरण किए गए अधिकतम वर्षण वाले क्षेत्रों का स्थान और तीव्रता, CNTL रन की तुलना में TRMM आँकड़ों से बेहतर मेल खाते हैं। CNTL रन अधिकतम वर्षा की तीव्रता का 1.6 सेमी से 50.6 सेमी तक की त्रुटियों के साथ अधिक आकलन करते हैं, जबकि SAT रन -2.6 सेमी से -19.1 सेमी तक की त्रुटियों के साथ तीव्रता का कम आकलन करते हैं। GPM आँकड़ों के साथ तुलना करके परिकलित सांख्यिकीय स्कोर, जैसे पूर्वाग्रह, क्रांतिक सफलता सूचकांक (CSI), और संसूचन की संभावना (POD), भी CNTL रन की तुलना में आत्मसातीकरण रन के वर्षा पूर्वानुमान में सुधार को उजागर करते हैं। अध्ययन में लघु-दूरी वर्षा पूर्वानुमान में सुधार करने में उपग्रह विकिरण समावेशन के महत्व को प्रस्तुत किया गया है।

ABSTRACT. This study deals with the assimilation of satellite radiances in improving the initial conditions of the Advanced Research Weather Research and Forecasting (ARW) model and its impact on the simulation of rainfall and other meteorological features associated with Monsoon depressions (MDs). Eight MDs occurring during 2015-2018 are considered for the study. A set of two numerical experiments: CNTL, which does not consider any data assimilation, and SAT, where satellite radiances are assimilated into the model initial condition, is conducted for each MD case. In this study, satellite radiance data from the sounding instruments Advanced Microwave Sounding Unit (AMSU), Microwave Humidity Sounder (MHS), and Atmospheric Infrared Sounder (AIRS) on polar satellites NOAA 15, NOAA 18, NOAA 19, EOS 2, METOP 1, and METOP 2 are used. The assimilation has been done using the region-specific background error statistics computed for June to August 2017 using the National Meteorological Centre (NMC) method.

Improvements in the tracks of MDs after assimilation are seen from 12h to 42h, with a minimum track error of 320 km for SAT runs, in contrast to 400 km for CNTL runs. Winds, mainly at upper tropospheric levels, were simulated well after assimilation, while for lower-level winds, assimilation runs are reliable for a longer range forecast (>24h). The assimilation runs capture both the intensity and spatial spread of precipitation better than the CNTL runs, compared to TRMM precipitation as well as with India Meteorological Department (IMD) station observations. Also, the location and intensity of the maximum precipitation regions simulated in SAT runs are in better agreement with TRMM data than CNTL runs. CNTL runs overestimate the intensity of maximum precipitation with errors from 1.6 cm up to 50.6 cm, while SAT runs underestimate the intensity with errors from -2.6 cm to -19.1 cm. The statistical scores, such as bias, critical success index (CSI), and probability of detection (POD), computed by comparing with GPM data, also highlight the improvement in precipitation forecast of the assimilation runs compared to the CNTL runs. The study presents the significance of satellite radiance assimilation in improving the short-range rainfall prediction.

Key words – Satellite radiance, Assimilation, Monsoon depressions, Indian region.

1. Introduction

The Indian summer monsoon (ISM) or the South Asian Monsoon is the strongest monsoon system in the world. Nearly one-sixth of the world population is dependent on it for their survival. The variation in ISM not only impacts the food and water resources of a region but also plays a crucial role in shaping the overall economy (Gadgil and Gadgil, 2006). The duration of ISM is generally from June to October, with a sudden onset at the beginning of June and slow withdrawal at the end of September or at the beginning of October. The Indian Summer Monsoon Rainfall (ISMR) is the major source of water for the Indian region, so the monsoon season and its associated rainfall have a large socioeconomic impact on the region's economy. Monsoon season contributes 70-80% of the total annual rainfall of India (Gadgil and Gadgil, 2006). During monsoon season, there are different rain-bearing systems, including offshore troughs, which produce rainfall along the west coast, mid-tropospheric circulations, which produce rainfall along the west coast of India and the northwest parts of India, and monsoon depressions (MDs). MDs are synoptic-scale disturbances that form in the monsoon circulation during the southwest monsoon season of June to September (Sikka, 1977; Hurley and Boos, 2015). It is an important rain-producing system of the monsoon. It is associated with widespread (Godbole, 1977; Mooley and Shukla, 1989) and heavy rainfall (Ajayamohan *et al*., 2010) in parts of central and northwestern India. So, a better understanding of it is necessary to simulate it well.

For short-range prediction, it is necessary to have accurate initial conditions, as the model performance is sensitive to perturbations in initial conditions. Improvements in initial conditions are possible with the incorporation and assimilation of high-resolution observations. Studies such as Routray *et al*. (2016) and Osuri *et al*. (2015) demonstrated that data assimilation provides better initial conditions to a numerical weather prediction (NWP) model. Most of the MDs form over the sea, a region where data availability is scarce. Observations from non-conventional sources such as satellites play a crucial role in providing information about the meteorological system. Studies such as Rakesh *et al*. (2010) have shown that the assimilation of satellite observations has improved model-predicted rainfall during the monsoon season.

In this study, the Advanced Research Weather Research and Forecasting (ARW) modelling system is used. A detailed description of model physics, dynamical core, and model equations of the ARW modelling system is given in Skamarock *et al*. (2005). Barker *et al*. (2004) described the practical implementation of the 3DVAR system along with results from the initial case study and its real-time application. Earlier studies have considered coarser resolution (Routray *et al*., 2013), which performed better in the study of large-scale features of the monsoon. Further, the model showed relatively higher errors in the quantitative prediction of rainfall associated with different rain-bearing systems of the monsoon season. Considering the MDs and associated rainfall activity, the resolution needs to be finer to capture the sub-grid scale processes. In recent years, voluminous data have been available from different satellites over different parts of the globe. A comprehensive objective of this study is to assess the impact of satellite radiances as a whole on the simulation of MDs and associated rainfall activity.

Section 2 describes an overview of experiments, data, and methodology. A brief description of the three-dimensional variational assimilation system is given in section 2.1. Section 2.2 explains the background error calculation, and Section 2.3 lists the datasets used. Results and analysis are presented in Section 3. It is divided into two parts: Impact of satellite radiance on initial condition (Section 3.1) and Impact on model simulations (Section 3.2). Section 4 consists of the conclusions.

2. Data and methodology

Eight MD cases that formed over the Bay of Bengal (BoB) in recent years (2014 – 2018) are considered. The brief synoptic features associated with the events are discussed in Table 1. These cases are simulated using the

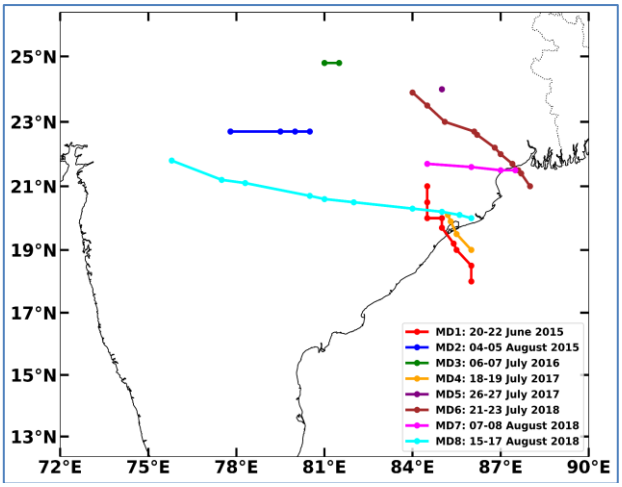

Fig. 1. The domain considered for the study and the tracks of MDs considered. The resolution of the domain is 4 km

ARW model with a single domain with 4 km horizontal grid spacing and 51 sigma levels. The vertical levels are placed finer in the lower atmosphere up to 700 hPa, which becomes coarser in the upper atmosphere.The physical and microphysical parameterizations include the New Thompson scheme for microphysics, the Tiedtke scheme for cumulus parameterization, the Mellor-Yamada-Janjic scheme for the Planetary Boundary Layer (PBL), the RRTM radiation scheme, the Eta similarity for surface layer physics, and the Noah land surface model for land surface. The domain considered for study and the tracks of the studied MDs are shown in Fig. 1. The 0.25° × 0.25° grid Global Forecast System (GFS) analyses and forecast products of the National Centers for Environmental Prediction (NCEP) are used to prepare the model initial and lateral boundary conditions. The lateral boundary conditions are updated in a 6 h interval from the GFS forecast fields.

A set of two numerical experiments is conducted. The first set, named CNTL, is carried out without any assimilation of satellite radiances. The second set of experiments (SAT) uses satellite radiance data to update the model's initial condition. Assimilation of radiance takes place over both land and sea. All the MD cases are initialized at different initial times for at least a 24 h forecast length; a total of 14 simulations are obtained. The list of the simulations, along with their forecast time, is given in Table 2. The simulations for different cases are performed with single or multiple initial conditions for a depression, depending on the lifetime of the depression. This is done to assess the influence of assimilation cycle timing on short-range forecasts and the performance of 3DVAR assimilation at different start times and forecast lengths in capturing variability in an evolving MD structure.

Satellite radiance measurements are prone to error, which must be regularly corrected before assimilating radiance observations. The most common method is variational bias correction (VarBC) that performs bias correction (BC) as a part of the analysis, thereby considering information from observations and the full background field. Derber and Wu (1998) and Dee (2005) have given a detailed description of the VarBC method.

2.1. *Three-dimensional variational data assimilation (3DVAR)*

The 3DVAR assimilation system within the ARW model framework is used. The main principle of this method is to avoid the computation of a gain matrix (K) by taking analysis as an approximate solution to the minimization problem. This is done by defining a cost function J, and the primary aim is to minimize the cost function by performing several iterations. Cost function is the sum of squared deviations of analysis values from observation values weighted by the accuracy of the observation, plus the sum of squared deviations of forecast fields from analysed fields weighted by the accuracy of the forecast (Equation 1). This helps in maintaining the analysis close to the observations. The cost function (J) is represented by:

$$J(X) = J^b + J^o = \frac{1}{2}(x - x^b)^T B^{-1}(x - x^b) + \frac{1}{2}(y - y^o)^T (E + F)^{-1}(y - y^o) \quad (1)$$

where $\mathbf{J^b}$ and $\mathbf{J^o}$ are the background and observation cost functions, $\mathbf{x}$ is the state vector, $\mathbf{x^b}$ is the first guess (or also known as background field), $\mathbf{B}$ is the background error covariance, $\mathbf{y}$ is the model state projected into observational space ($\mathbf{y=Hx}$), $\mathbf{H}$ is the nonlinear forward operator, $\mathbf{y^o}$ is the observation, $\mathbf{E}$ is the observational or instrumental error covariances, and $\mathbf{F}$ is the representative error covariances.

The minimization can be stopped by limiting the number of iterations or when the gradient decreases to a predefined amount. This is a measure of how close the analysis is to the optimum from the initial point before minimization. Compared to other methods, the variational assimilation allows greater flexibility in assimilating different types of data. The main advantage of this method is to remove the local data selection as seen in optimum interpolation (OI) method (Eyre, 1987), and allows to perform a global analysis. So this method eliminates the problem of splitting the domain into subdomains so that all observations can influence analysis at every grid point of the study domain. It also provides a general framework for handling complex background-error covariance. The popularity of 3D-Var is due to its conceptual simplicity &

TABLE 1

Synoptic Features of Monsoon depressions considered in the study

Sl.No.	MD PERIOD	SYNOPTIC FEATURES
1	20-22 June 2015	Genesis of the depression is on 20th June 2015 at 03 UTC northwest and adjoining west central BoB near 18.0° N/86.0° E Crossed Odisha coast between Gopalpur and Puri around 20-21 UTC on 20th June Estimated central lowest pressure is 990 hPa and maximum wind speed is 25 knots at 03 UTC of 20th June near 18.0° N/86.0° E
2	04-05 August 2015	Genesis of the depression is on 04th August 2015 at 03 UTC over East Madhya Pradesh and adjoining Chhattisgarh near 22.7° N/80.5° E Weakened into a well-marked low pressure area over southwest Madhya Pradesh and neighbourhood at 00 UTC on 5th Aug. Estimated central lowest pressure is 998 hPa and maximum wind speed is 25 knots at 03 UTC on 4th Aug. A remnant of cyclonic storm 'KOMEN' which developed as a well- marked low and then strengthened into a depression at 03 UTC of 4th Aug. It moved westward and weakened into a well-marked low pressure area around 00 UTC of 5th Aug.
3	06–07 July 2016	Genesis of the depression on 6th July 2016, 03 UTC over north Madhya Pradesh and neighbourhood near 24.8° N/81.5° E Weakened in to a well-marked low pressure area over northeast Madhya Pradesh and neighbourhood at 03 UTC on 7th July Estimated central lowest pressure is 996 hPa and maximum wind speed is 25 knots at 03 UTC of 6th July near 24.8° N/81.5° E It caused heavy to very heavy rainfall over Madhya Pradesh and adjoining areas of Maharashtra.
4	18–19 July 2017	Genesis of the depression on 18th July, 2017, 00 UTC over northwest and adjoining westcentral BoB and coastal areas of Odisha near 19.0° N/86.0 °E Weakened into a well-marked low pressure area over interior Odisha and neighbourhood at 03 UTC on 19th July Estimated central lowest pressure is 992 hPa and maximum wind speed is 25 knots at 00 UTC of 18th July near 19.0° N/86.0° E It moved west-northwestwards and crossed Odisha coast near Puri around 20:30 hours IST on 18th July and continued to move in the same direction and weakened gradually
5	26–27 July 2017	Originated over Jharkhand and neighbourhood centered near 24.0° N/85.0° E at 00 UTC on 26th July 2017 Depression weakened into a well-marked low pressure area over northeast Madhya Pradesh and neighbourhood at 03 UTC of 27th July Estimated central lowest pressure is 993 hPa and maximum wind speed is 25 knots at 00 UTC on 26th July Active monsoon condition across central part of the country with intense rainfall activity over this region.
6	21–23 July 2018	Genesis of the depression on 21st July 2018, 03 UTC over northwest BoB near 21.0° N/88.0° E Weakened into a well-marked low pressure area over northwest Jharkhand and neighbourhood at 03 UTC 23rd July Estimated central lowest pressure is 989 hPa near 21.0° N/88.0° E with maximum wind speed of 25 knots at 03 UTC 21st July It had a straight moving track and a life period of 48 hours.
7	07–08 Aug 2018	Genesis of the depression on 7th August 2018, 09 UTC over northwest BoB near 21.5° N/87.5° E Depression weakened into a well-marked low pressure area over north Chattisgarh and neighbourhood at 03 UTC of 8th August Estimated central lowest pressure is 992 hPa and maximum wind speed is 25 knots at 09 UTC 7th August near 21.5° N/87.5° E
8	15–17 Aug 2018	Genesis of the depression on 15th Aug 2018, 03 UTC over coastal Odisha near 20.0°N/86.0°E Weakened into a well-marked low pressure area over southwest Madhya Pradesh and adjoining Gujarat & north Madhya Maharashtra Estimated central lowest pressure is 993 hPa and maximum wind speed is 25 knots at 03 UTC 15th Aug near 20.0° N/86.0° E

(*Source: IMD RSMC Reports***)**

TABLE 2

Simulations and their forecast length

Simulation number	Initial condition	Forecast length(h)
1	15.08.2018 : 00 UTC	48
2	15.08.2018 : 12 UTC	36
3	16.08.2018 : 00 UTC	24
4	07.08.2018 : 00 UTC	24
5	21.07.2018 : 00 UTC	48
6	21.07.2018 : 12 UTC	36
7	22.07.2018 : 00 UTC	24
8	26.07.2017 : 00 UTC	24
9	18.07.2017 : 00 UTC	24
10	06.07.2016 : 00 UTC	24
11	04.08.2015 : 00 UTC	24
12	20.06.2015 : 00 UTC	48
13	20.06.2015 : 12 UTC	36
14	21.06.2015 : 00 UTC	24

TABLE 3

Assimilated satellite data for each case

Simulation	Noaa 15 Amsua	Noaa 18 Amsua	Noaa 18 Mhs	Noaa 19 Mhs	Eos 2 Airs	Metop 1 Mhs	Metop 2 Mhs	Metop 2 Amsua
1	*	*	*	*	*			
2	*	*	*	*		*		
3	*	*	*	*				
4	*	*	*	*				
5	*	*	*	*				
6	*	*	*	*				
7	*	*	*	*				
8	*	*	*	*				
9	*	*	*	*	*			
10	*	*	*	*	*			
11	*	*	*	*			*	
12	*	*	*	*				
13	*	*	*				*	*
14	*	*	*	*				

the way complex observation operators are used. In OI, we need to specify the background error covariance model between each observed and model variable, which makes this method complicated (Parrish & Derber, 1992; Courtier *et al*., 1998).

In 3DVAR, observations make local, isotropic increments without proper flow-dependent extrapolation and the background error covariances do not automatically adjust with observation networks. So, the results from this data assimilation method are dependent on the number and types of observations assimilated (Kutty & Wang, 2015).

2.2. *Background error calculation*

Background error statistics (BES) play an important role in spreading the observations spatially and filtering analysis increments based on dynamical balances and statistical relationships (Courtier *et al*., 1998). In observation-sparse regions, especially over oceans, the background field provides a more realistic analysis as the model includes the physics and dynamic processes. Simple interpolation of observations might produce erroneous results as the interpolation efficiency decreases with distance, and the physics and dynamics are also not taken into consideration.

In this study, we have used the National Meteorological Centre (NMC) method for calculating the Background Error covariances (BEC). The NMC method (Parrish and Derber, 1992) approximates the BES using the difference of two model forecasts having different initial times but are valid at the same time. This gives insight into the numerical model itself. This method uses a control variable transform (CVT) that converts the model variables into control variables of the assimilation system. BEC used in this study is calculated for the domain shown in Fig. 1 using the region-specific CV5 option. 12 and 24-hour forecasts were generated from June 2017 to August 2017 at 00 UTC and 12 UTC. Perturbations were calculated between the 12 and 24-hour forecasts valid at the same time. The average of the perturbations is calculated to generate the BEC for the monsoon season. Routray *et al*. (2014) showed that the use of regional BES in the assimilation cycle has a positive impact on the prediction of location, propagation, and development of rainbands associated with MDs. Initial conditions also improved through assimilation of observations and using domain-dependent BES.

2.3. *Datasets used*

NCEP Global Forecast System (GFS) with a 0.25° × 0.25° global latitude longitude grid is used to provide the boundary conditions for the model run. Model forecast runs are done at 00, 06, 12, and 18 UTC daily. The grids include analysis and forecast time steps at a 3-hourly run from 0 to 240 hours and at a 12-hourly interval from 240 to 384 hours. NCEP Global Data Assimilation System (GDAS) datasets contain subsets of level 1b or higher satellite data products that can be used in NCEP GDAS systems. They have a lot of applications, especially in areas where conventional observations are scarce. The datasets assimilated in the simulations of each case are given in Table 3. Here, blank entries under a specific platform indicate unavailability of satellite overpasses within the assimilation window or exclusion due to quality control (QC) threshold rejections (e.g., high cloud contamination, limb effects).

Satellite radiance data from the sounding instruments Advanced Microwave Sounding Unit (AMSU), Microwave Humidity Sounder (MHS), and Atmospheric Infrared Sounder (AIRS) on polar satellites NOAA 15, NOAA 18, NOAA 19, EOS 2, METOP 1, and METOP 2 are used. A higher number of AMSU observations are assimilated as compared to other satellite radiances. The simulation of surface-sensitive channels of AMSU observations may be affected by the inaccurate

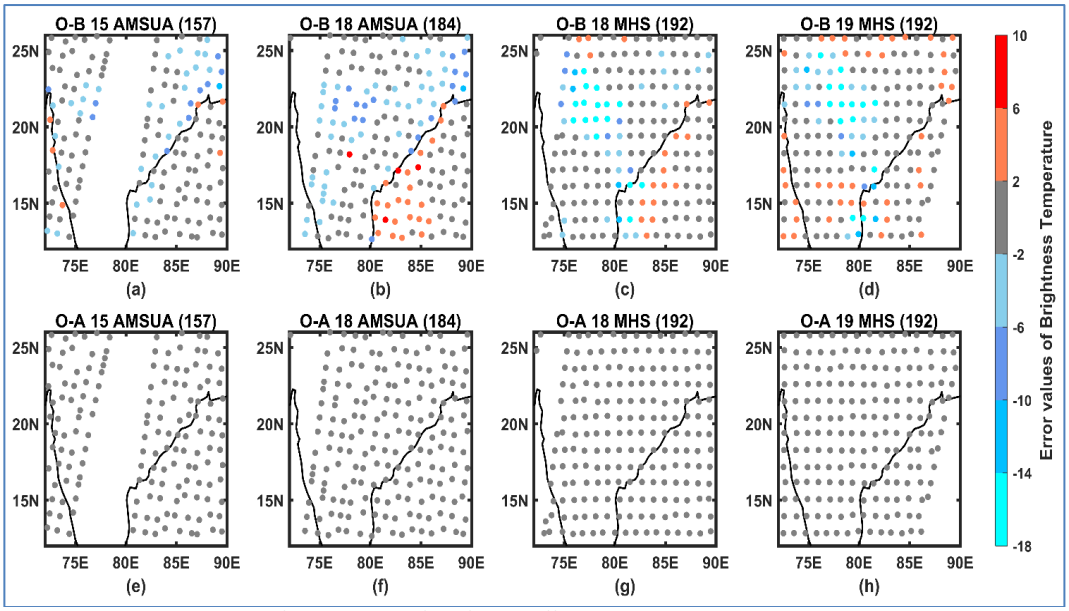

Figs. 2. (a-h);(a-d) Background field departure of BT for the different satellite radiances assimilated in simulation 11; (e-h) Analysis departure of BT for different satellite radiances assimilated in the same simulation. The quantity in the bracket represents the number of observations assimilated

representation of skin temperature and surface emissivity (Karbou *et al*., 2006). These quantities are derived from the background information. Accurate representation of background information plays an important role in determining the impact of AMSU observations, and this effect is generally more prominent in the northern hemisphere (NH), which has a higher land surface coverage.

Tropical Rainfall Measuring Mission (TRMM) 3-hourly and daily datasets are used to compare with the model rainfall. TRMM 3B42 is a fine-scale (0.25° × 0.25° and 3-hourly) satellite-determined precipitation dataset accessible in the latitude band 50°S – 50°N. The TRMM 3B42 precipitation-related passive microwave data are mainly collected by a series of satellites in low Earth orbit, while the infrared data are gathered in a window channel (~10.7 μm) by an international constellation of Geosynchronous Earth Orbit (GEO) satellites. Half-hourly Integrated Multi-satellitE Retrievals for Global Precipitation Measurement (IMERG) (Huffman *et al*., 2014) datasets are used to compare the skill metrics of precipitation estimates. These Global Precipitation Measurement (GPM) L3 "Final" products are computed at 0.1° × 0.1° resolution using data from precipitation-measuring satellites and other data, including monthly surface precipitation gauge analyses.

Other meteorological fields simulated by the models are compared with the fifth generation European Centre for Medium-Range Weather Forecasts (ECMWF) reanalysis (ERA5) datasets with a spatial resolution of 0.25° × 0.25° (Hersbach *et al*., 2020). The data is used for comparison with model outputs such as mean sea level pressure, winds, vertical profiles of temperature, and specific humidity. The best track data for the IMD Regional Specialised Meteorological Centre (RSMC) is used to track MDs.

3. Results and discussions

The impact of assimilating satellite radiances on MD simulations is discussed in this section. Simulations numbered 11, 12 of cases 1 and 2 are used to show the individual impacts on assimilating satellite radiances. Impact of assimilation on initial conditions, 10-m winds, winds at different pressure levels, track predictions, vertical profiles, and distribution of model-simulated rainfall are also analyzed.

3.1. *Impact of satellite radiance on initial condition*

Figs. 2(a-d) represents the background field departure (difference between model brightness temperature (BT) before assimilation with the observed BT) for different satellite radiances assimilated in run 11. Figs. 2(e-g) represents the assimilated field departure (difference between model BT after assimilation with the observed BT) for different satellite radiances assimilated in the same simulation. The negative values indicate that the background or analysis fields show a greater value of BT compared to observations. Background field departures are higher mainly over regions of central India and the BoB, and the boundaries of the domain (for MHS

assimilation). The background field departures have been considerably reduced after assimilation of satellite radiances. Major improvements can be seen over central India and the eastern BoB. The error range has considerably reduced, and it ranges between -2 and +2 after assimilation.

A scatter plot is plotted between observed BT after BC with background (Fig. 3a) and analysis BT (Fig. 3b) with the colours representing different types of radiance data assimilated. Correlation coefficient and RMSE values are given in Table 4. There is a substantial improvement in all the correlation coefficients, particularly of NOAA MHS-18, 19, followed by METOP 2 MHS after assimilation. RMSE values are also significantly reduced after assimilation. The maximum reduction in RMSE value is seen for NOAA MHS 18 from 13.82 to 0.26, followed by NOAA MHS 19 from 9.15 to 0.21. These significant improvements are due to the assimilation of high-quality radiance channels, particularly in temperature- and humidity-sensitive bands over the depression's location.

Vertical profiles of wind speed, temperature, and specific humidity are shown in Fig. 4. Vertical profiles are calculated for a $2^{o} \times 2^{o}$ box from the centre of the MD. Fig. 4(a-c) represents the profiles for simulation 11 (04.08.2015 00 UTC). Fig. 4(d-f) represents the vertical profiles for simulation 12 (20.06.2015 00 UTC). The profiles of the SAT runs show an overall better agreement with the profiles of ERA5 for both cases, in general. Major improvements can be seen in the simulation of temperature and specific humidity profiles of SAT runs, *i.e*., closer to the observation profile in the boundary layer (below 700 hPa). This suggests that the SAT runs represent the cold core of MDs well and simulate a relatively moister atmosphere, approximately till mid-troposphere, closer to ERA5 profiles. Whereas, the CNTL runs simulate a relatively drier atmosphere.

Figs. 5(a-c) represents the mean bias for vertical profiles of wind speed, temperature, and specific humidity, respectively. As shown in Fig. 5(a), the biases of the CNTL and SAT runs for wind speeds are similar. However, for temperature and specific humidity, it is observed that the bias for SAT runs is lower than that for CNTL runs till mid-troposphere. While at higher levels, *i.e*., 400-500 hPa and above, the biases for both experiments are nearly equal. There has been a significant improvement in profiles of temperature and moisture, especially in layers between 500 hPa and 1000 hPa.

3.2. *Impact on model simulations*

Model simulated tracks for simulations 1, 9, 11 and 12 are shown in Figs. 6(a-d). IMD best track data is also shown for reference. SAT runs give a better prediction of MD tracks. The positional error for 3DVAR runs is less for the reference cases shown. SAT runs are also able to capture the north-northwestward movement of MDs. The variation of mean track error with forecast length for both experiments shows that initially, for a forecast length of up to 9 hours, CNTL runs produce better simulations of MD tracks (Fig. 6e). However, as the forecast length increases, there is a considerable reduction in mean track errors of SAT runs than CNTL runs, with values ~500, 480, 420 and 700 km for the SAT runs and ~650, 580, 520 and 650 km for CNTL runs at 12h, 24h, 36 h & 48h respectively. The minimum track error obtained in SAT runs is 320 km, in contrast to 400 km for CNTL runs at 42h. The intensity in terms of maximum wind speed at 10 m shows that SAT runs have overall higher prediction skill than CNTL runs throughout the simulation length (Fig. 7).

Fig. 8 shows the 12-hour forecast of wind speeds at 850 hPa [Figs. 8(a-c)], 500hPa [Figs. 8(d-f)], and 10 m [Figs. 8(g-i)] for simulation 11. The CNTL and SAT runs are compared with the ERA5 reanalysis dataset. At 850 hPa [Figs. 8(a-c)], the model runs are predicting the circulation patterns well; however, the intensity, mainly in the southern sectors, is underestimated, mainly in the SAT run compared to the reanalysis data. The strong winds on the south-western sector at 500 hPa are highly underestimated in both runs. The circulations at 500 hPa and 10 m are slightly better defined in SAT runs. There is an improvement in the circulation pattern at 10m, which is scattered for the CNTL run, but slightly better defined in the SAT run. An important feature during MD intensification is the presence of strong lower tropospheric westerlies at 850-900 hPa (Krishnamurty and Bhalme, 1976). This feature was simulated well in both model runs.

The mean RMSE of wind speed at 850 hPa and 500 hPa of the simulations is plotted in Fig. 9 as a function of forecast length. For lower-level winds (Fig. 9a), assimilation runs are reliable for a longer range forecast (>24h) due to their lower RMSE values. Initially, for a forecast length up to 24h, CNTL runs show lower RMSE values and are more reliable, which is also seen in the circulation patterns at 12h (Fig. 8a). RMSE values for upper-level winds (500hPa) are shown in Fig. 9(b). For the entire forecast range, assimilation runs are more reliable and have lower RMSE values than CNTL runs, which matches the results of the circulation patterns at 12h (Fig. 8b). Hence, large impacts of assimilating satellite radiances can be noticed in upper tropospheric levels as compared to the lower levels. The result obtained is consistent with the studies Zapotocny *et al*. (2008) and Kutty and Wang (2015). In this study channels 5 to 9 for

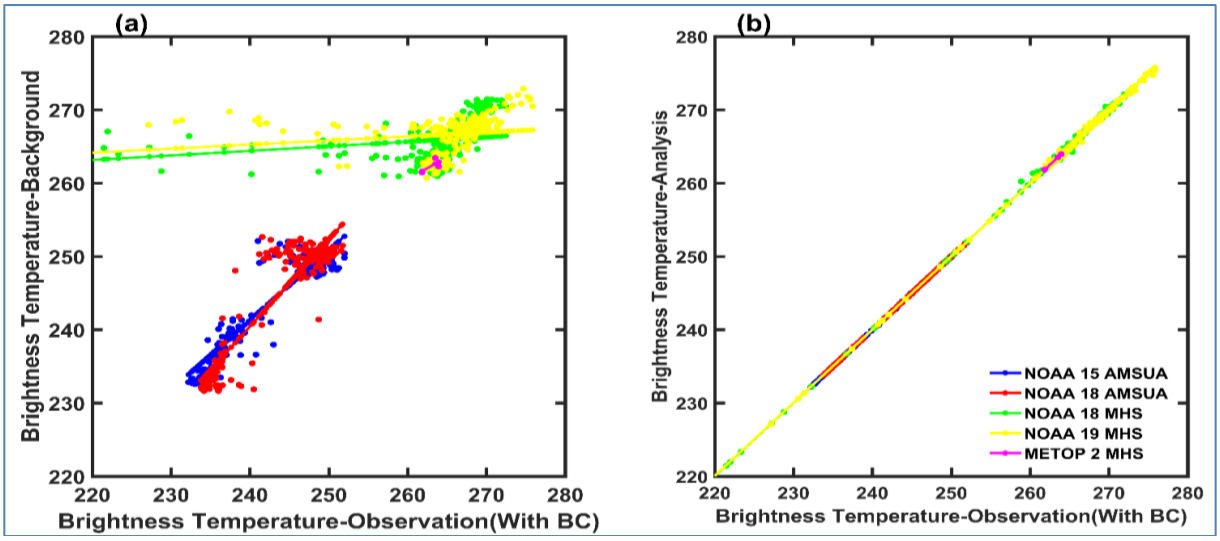

Figs. 3(a&b). Scatter plot between the observational BT and model BT before and after assimilation

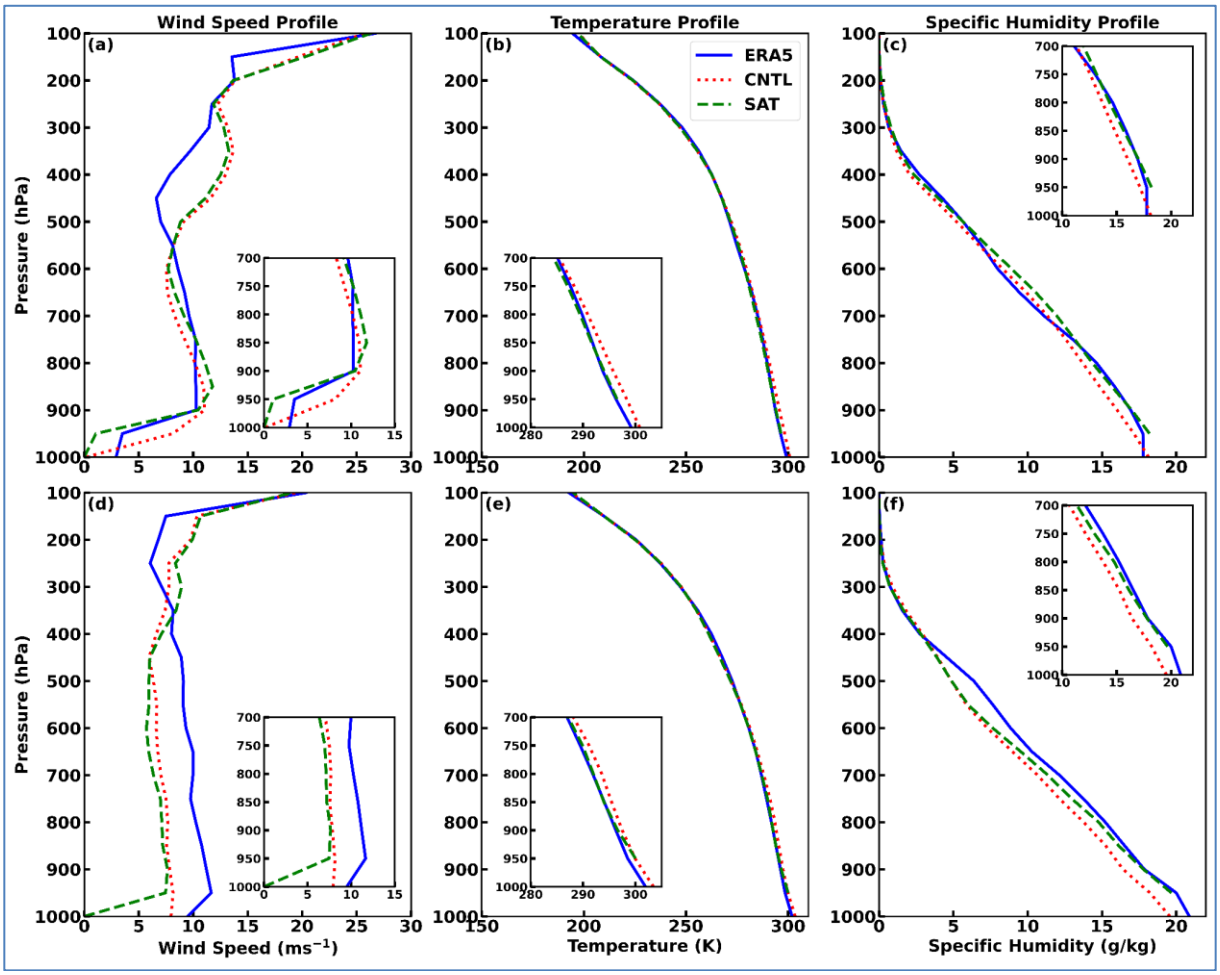

Figs. 4(a-f); (a-c) Vertical Profiles of wind speed, temperature, and specific humidity on 04.08.2015 00 UTC (I.C. of simulation 11); (d-f) Vertical Profiles of wind speed, temperature, and specific humidity on 20.06.2015 00 UTC (I.C. of simulation 12)

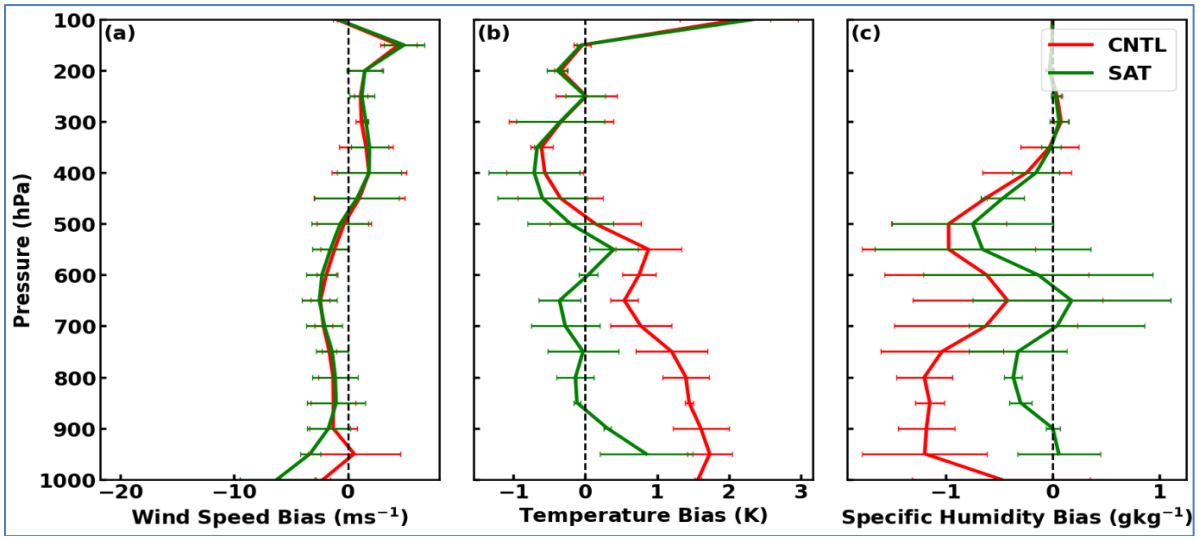

Figs. 5(a-c) Mean bias (CNTL Run– OBS and SAT- OBS) for vertical profiles of (a) wind speed, (b) temperature, and (c) specific humidity

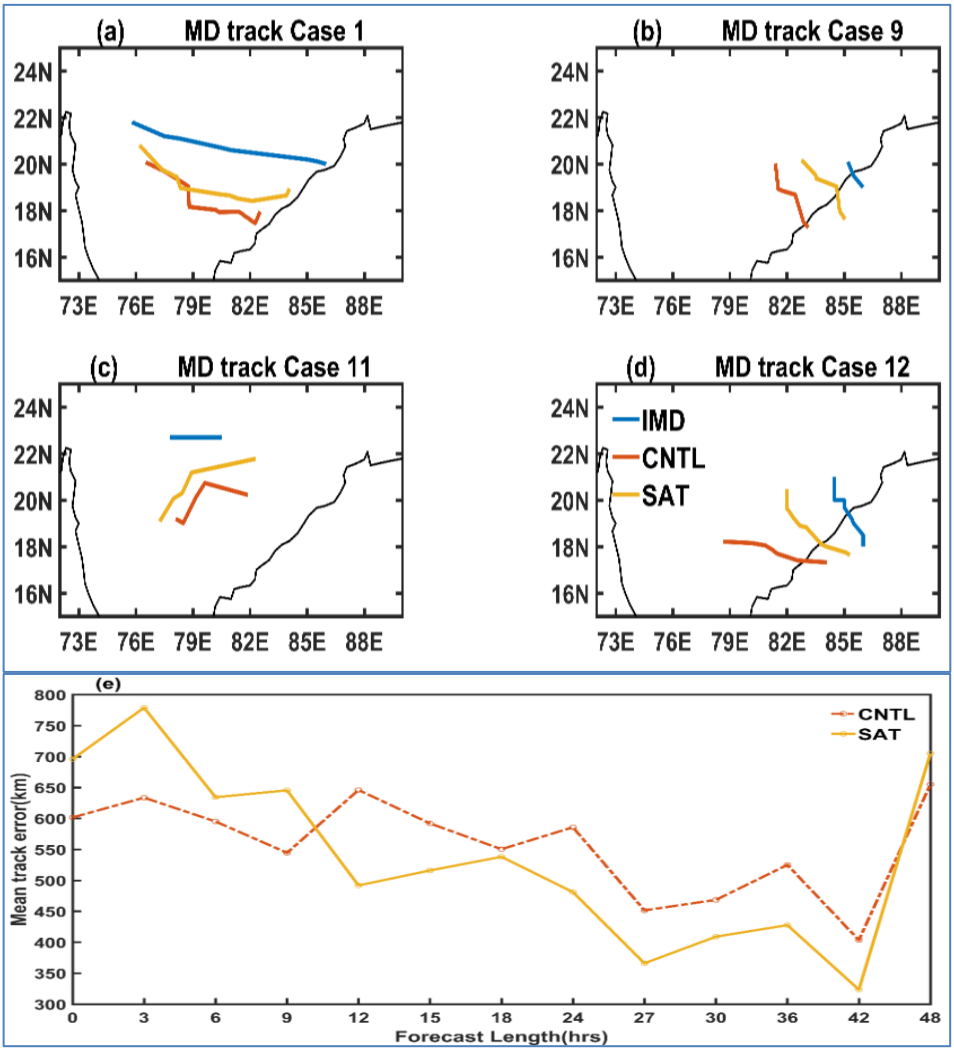

Figs. 6(a-e): (a-d) Forecasted track for CNTL and 3DVAR runs along with IMD best track data for simulations 1, 9, 11 and 12, (e) Time series of mean track error

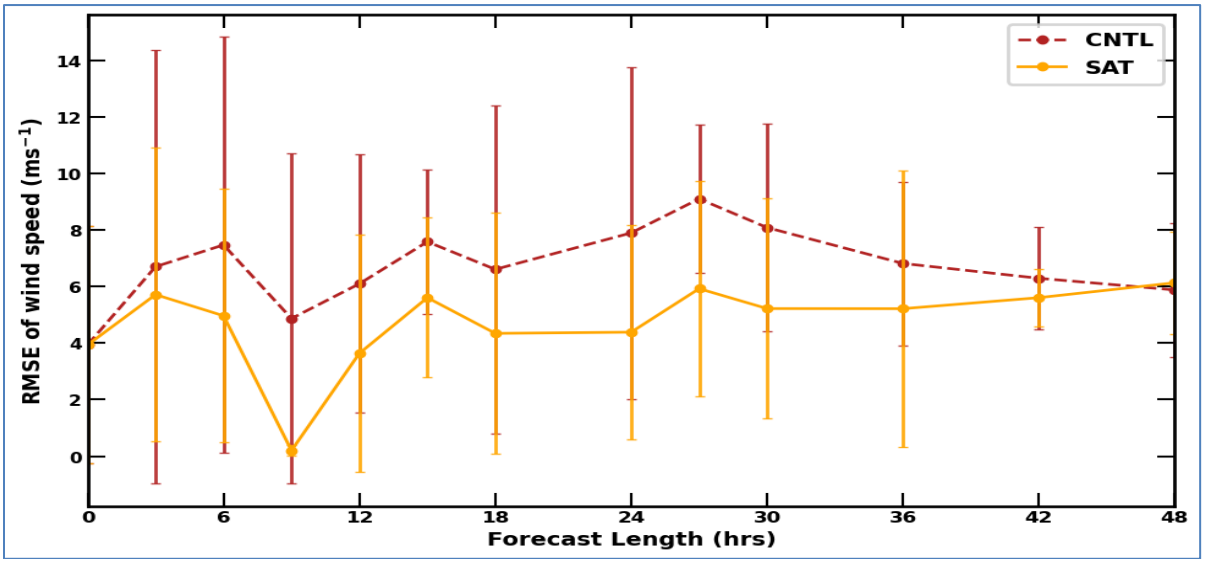

Fig. 7(a). Time series of RMSE of maximum wind speed at 10m as a function of forecast length. Different lines represent CNTL and SAT runs

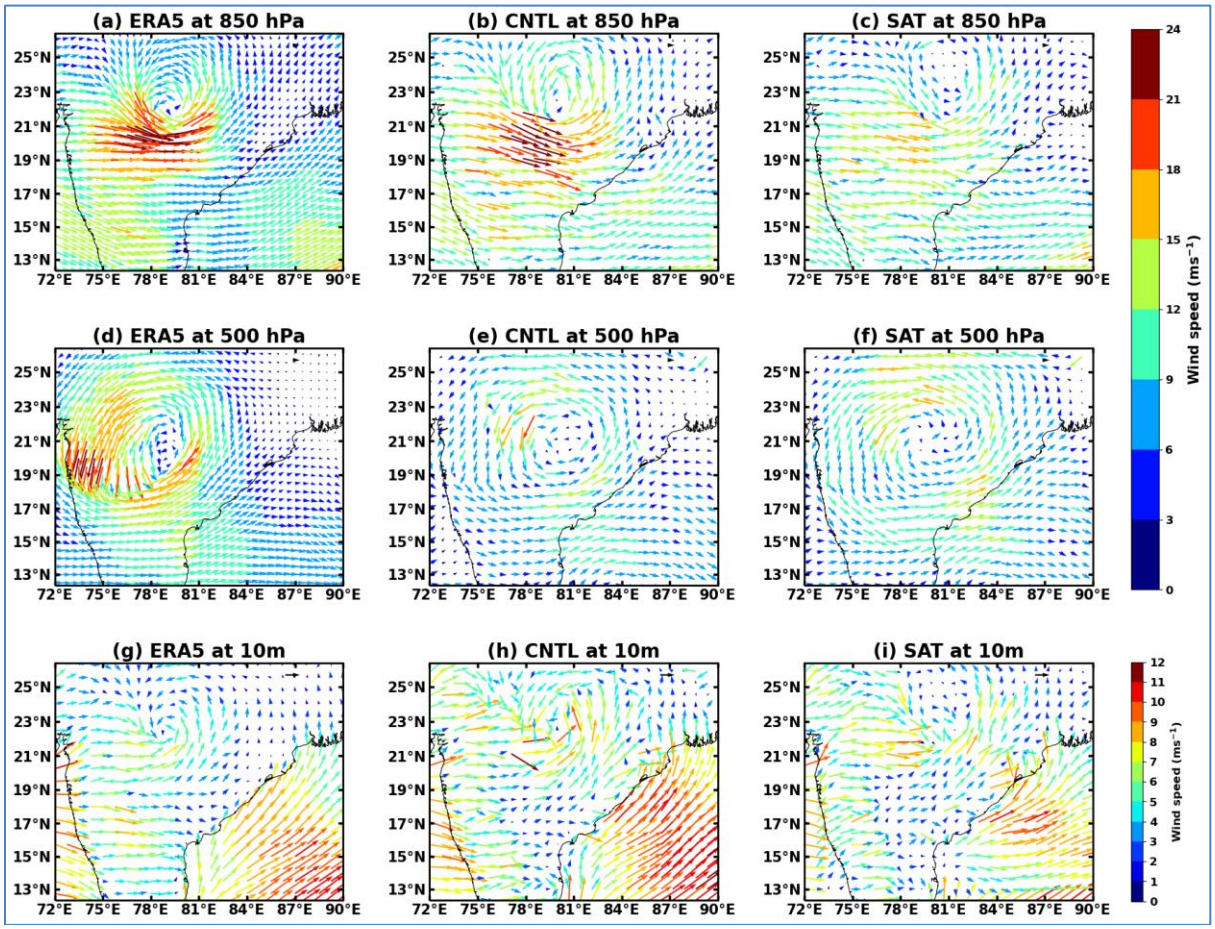

Figs. 8(a-i). Represent 12 hour forecast of winds at (a-c) 850hPa, (d-f) 500hPa, and (g-i) 10m for case 11 (IC: 04.08.2015: 00 UTC) for ERA5, CNTL, and SAT runs, respectively

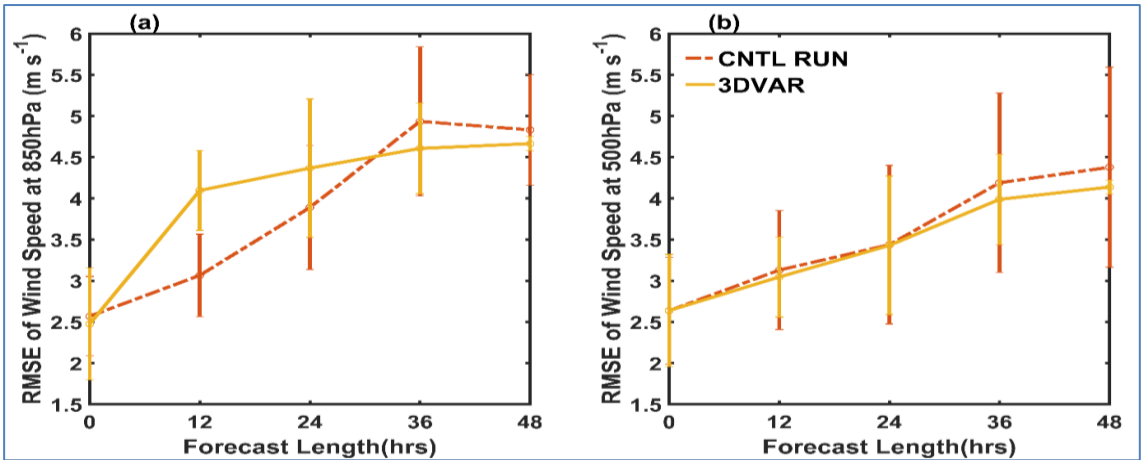

Figs. 9(a&b). Mean RMSE of wind speeds at (a) 850hPa and (b) 500hPa as a function of forecast length

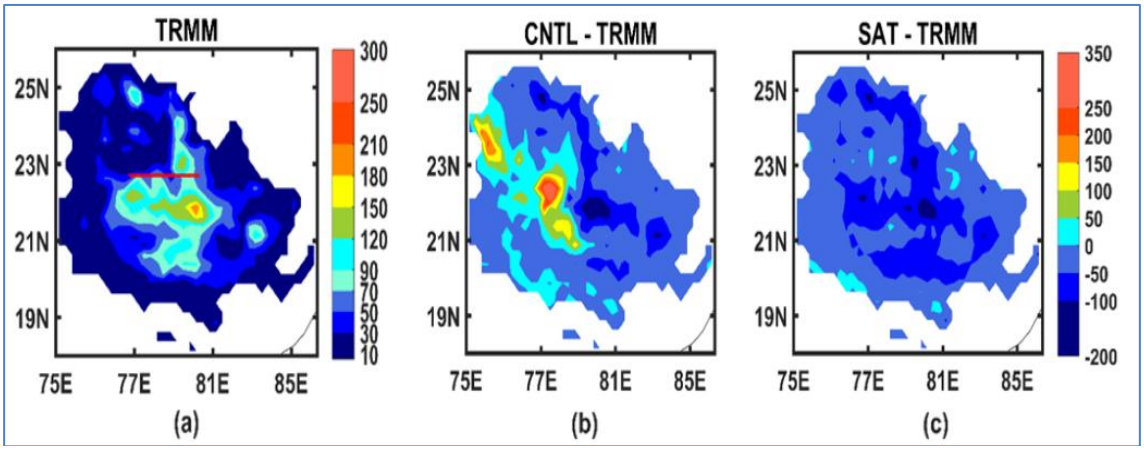

Figs. 10(a-c). Total precipitation on 04.08.2015 (Simulation 11) in mm from TRMM data. The red line represents the track of the depression. Difference between: (b) CNTL and TRMM precipitation, and (c) SAT and TRMM precipitation, respectively, in mm

AMSU-A and channels 3 to 5 for MHS are assimilated for temperature and moisture fields. So, the poor performance of assimilation runs in the lower troposphere may be attributed to the fact that the channels that detect the meteorological fields in the lower troposphere are not assimilated.

Model-simulated 24h rainfall from CNTL and SAT experiments is compared with the TRMM captured rainfall for simulation 11 (Fig. 10). Rainfall obtained from TRMM data is shown in Fig. 10(a). Figs. 10(b&c) show the difference between TRMM rainfall analysis and model values in mm. Positive values indicate model runs simulate a higher precipitation intensity, while negative values indicate underestimation by model runs. The CNTL run (Fig. 10b) overestimates the intensity of precipitation, with an error range between 350 mm and -200 mm. While the SAT run (Fig. 10c) slightly underestimates the intensity of precipitation, with values ranging between 50 mm and -50 mm. The spatial spread of rainfall, however, is captured in the SAT run better than in the CNTL run. Thus, the assimilation run captures both the intensity and spread of rainfall better than the CNTL run.

Table 5 compares CNTL and SAT simulated rainfall at different stations with IMD observed rainfall values for case 11 on 04.08.2015. Both runs underestimate the precipitation intensity. The underestimation, in general, is higher for control runs than SAT runs, except at Chindwara, where CNTL overestimates precipitation than observations. CNTL's unrealistically strong convection that led to the overestimated rainfall is adjusted by 3DVAR assimilated moisture fields, leading to closer agreement in spatial distribution but a slight underestimation in magnitude. The values simulated by assimilation runs are, however, closer to the observed values. The location and intensity of maximum precipitation from TRMM rainfall data are given in Table 6 for all depression cases. In addition, location error and

TABLE 4

Correlation values and RMSE of background and analysis BT against observation BT values

RADIANCE ASSIMILATED	BACKGROUND		ANALYSIS	
	CORRELATION	RMSE	CORRELATION	RMSE
NOAA AMSUA 15	0.93	2.67	1.00	0.03
NOAA AMSUA 18	0.91	3.49	1.00	0.04
NOAA MHS 18	0.29	13.82	0.98	0.26
NOAA MHS 19	0.19	9.15	0.97	0.21
METOP 2 MHS	0.63	0.99	1.00	0

TABLE 5

Comparison of CNTL and 3DVAR simulated precipitation with IMD observed rainfall at different stations on 04.08.15

STATION	DATE	LATITUDE	LONGITUDE	IMD RAINFALL (cm)	CNTL RUN (cm)	3DVAR RUN (cm)
Amarwara	04.08.2015	22.29°	79.16°	15	4.09	4.43
Seoni - AWS	04.08.2015	22.08°	79.54°	12	4.12	3.99
Chindwara	04.08.2015	22.05°	78.93°	12	14.12	9.85
Keolari	04.08.2015	22.37°	79.9°	11	1.88	2.34
Katangi	04.08.2015	21.77°	79.8°	11	3.65	7.37
Lakhnadon	04.08.2015	22.6°	79.6°	10	4.08	5.83
Bemetara	04.08.2015	21.71°	81.53°	12	0.49	1.99
Raigarh	04.08.2015	21.89°	83.39°	7	0.69	0.8

magnitude error of maximum precipitation for CNTL and SAT runs for all cases are also included in the table. It is evident that for most cases, the location error and magnitude error of maximum rainfall are less for the SAT run. For all the cases, CNTL runs overestimate the intensity of maximum precipitation while SAT runs underestimate the intensity, but it is much closer to the TRMM value. However, the improved location error but with an underestimated magnitude implies that assimilation improves storm positioning by accurately representing low- and mid-level wind fields, which directly influences rainfall location, but intense precipitation cores remain underpredicted, possibly due to conservative moisture adjustments by the 3DVAR assimilation system or smoothing effects inherent to it. The assimilation of observations has helped improve the accuracy of capturing the location and magnitude of maximum precipitation. While all assimilated channels show improvement, AMSUA and MHS water vapor channels contribute most to rainfall forecast improvement due to their sensitivity to tropospheric moisture, which is crucial for MD dynamics.

Fig. 11 shows the mean absolute error of precipitation for different stations when the model values are compared with observed IMD rainfall values, with error values divided into different intervals. The error is divided into different intervals, and the error intervals are represented using different colours. A total of 105 stations were considered. The distribution of stations in different error intervals for the CNTL and SAT runs is given in Table 7. In assimilation runs, a higher percentage of stations are in the error range of 0-8 mm, and there is a significant decrease in the percentage of stations as the error range increases. In the case of CNTL, the error range of 8-15mm has a higher number of stations. Comparing both runs, it is evident that assimilation runs have higher stations in a lower error range, while in CNTL runs, more stations can be found in a higher error range, indicating that the assimilation of satellite radiances has resulted in a significant decrease in error values.

Model precipitation data is compared with Global Precipitation Measurement (GPM) half-hourly data to calculate skill metrics such as bias, critical success index (CSI), and POD (probability of detection). The skill scores are calculated using the contingency matrix, taking into consideration whether a forecast occurs or not (Wilks, 2011). CSI estimates how well an event is forecasted. The BIAS score calculates the ratio of the number of forecast events to the number of observed events, giving an idea of whether the model is over-predicting or under-predicting. A BIAS score of 1 means the model values are in agreement with observed values. POD gives the fraction of rainfall events that are correctly forecast.

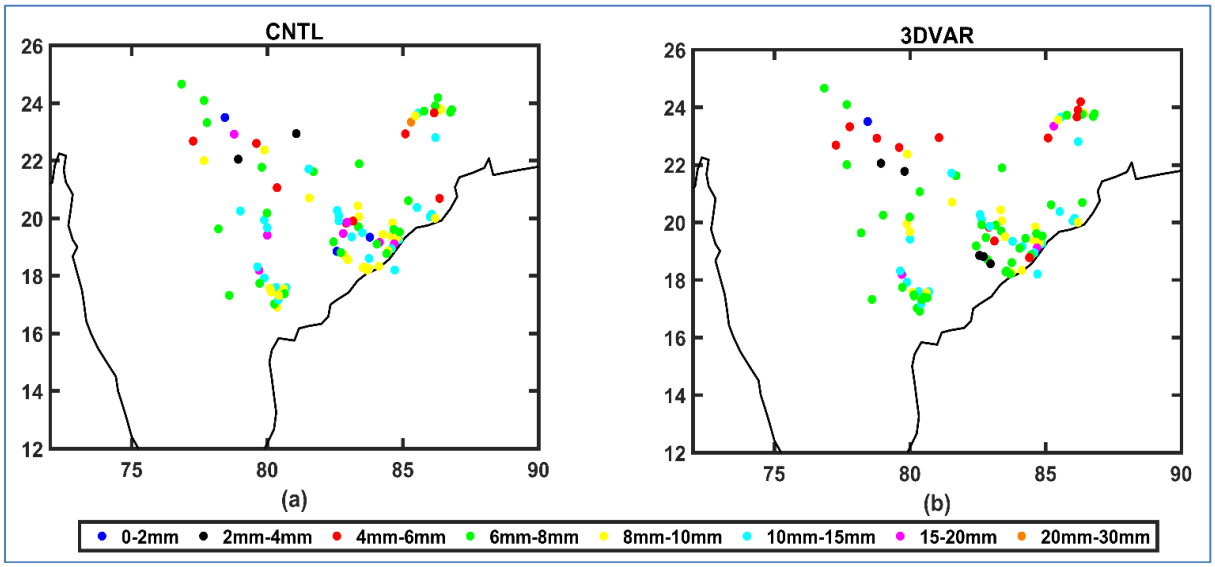

Figs. 11(a&b). Mean absolute error of precipitation for different stations when compared to IMD rainfall for CNTL and 3DVAR/SAT runs, respectively

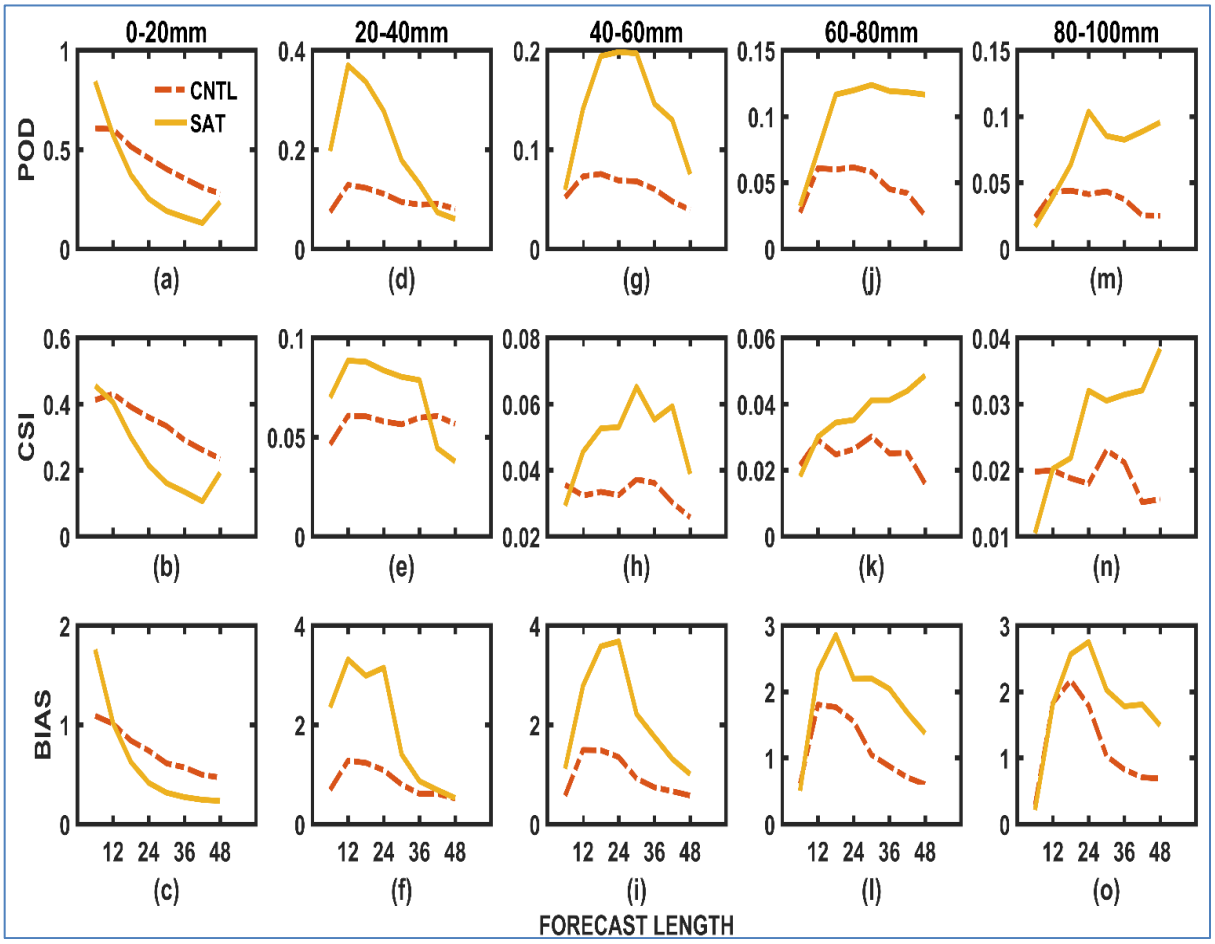

Figs. 12(a-o). Mean precipitation skill scores POD, CSI, BIAS for rainfall thresholds 0-20 mm (a-c), 20-40 mm (d-f), 40-60 mm (g-i), 60-80 mm (j-l), 80-100 mm (m-o), respectively

TABLE 6

Location and Intensity of maximum precipitation obtained from TRMM rainfall data, along with the location error and magnitude error of maximum precipitation for CNTL and 3DVAR runs for all depression cases

CASES	TRMM		CNTL		3DVAR	
	Location of maximum rainfall	Magnitude error of maximum rainfall (cm)	Location error of maximum rainfall (km)	Magnitude error of maximum rainfall (cm)	Location error of maximum rainfall (km)	Magnitude error of maximum rainfall (cm)
1	17.87° N 85.87° E	20.5	548	17	158	-6.3
2	18.62° N 79.87° E	21.3	180	12.9	460	-6.4
3	18.62° N 79.87° E	21.3	362	18.1	172	-9.6
4	19.62° N 87.37° E	17.7	439	11.9	327	-10.3
8	22.87° N 85.12° E	18.1	783	3.8	379	-6.6
9	18.12° N 84.12° E	20.5	253	16.1	300	-3.3
10	23.87° N 78.12° E	29.4	305	12.3	260	-19.1
11	21.87° N 80.37° E	20.4	204	50.6	199	-5
12	17.12° N 84.12° E	32.8	101	1.6	373	-7.8
13	17.87° N 84.62° E	18	299	49	433	-2.6
14	17.87° N 84.62° E	18	371	45	302	-4.4

TABLE 7

Distribution of stations in different error intervals

	Number of stations in the model runs with different error range	
Rainfall error range	CNTL RUN	3DVAR
0-2 mm	4	2
2-4 mm	3	7
4-6 mm	9	14
6-8 mm	29	42
8-10 mm	29	17
10-15 mm	23	20
15-20 mm	7	3
20-30 mm	1	0

Fig. 12 represents the mean precipitation skill scores for different rainfall thresholds. Figs. 12(a-c), (d-f), (g-i), (j-l), and (m-o) represent the mean skill scores for the intervals 0-20 mm, 20-40 mm, 40-60 mm, 60-80 mm, and 80-100 mm, respectively. SAT runs show a slightly higher bias value compared to the CNTL runs, indicating overestimation. The bias is higher for higher thresholds of rainfall, indicating that SAT runs overestimates precipitation for higher thresholds. SAT runs have higher bias values for initial forecast (< 24h), and the bias values approach 1 for longer forecast durations. Initially, CNTL runs show bias values close to 1, but it tends to underestimate as the forecast length increases. Except for the threshold of 0-20 mm, CSI scores for SAT runs are higher than those of CNTL runs. So, assimilation runs show a better skill in forecasting an event. POD values for CNTL runs are mostly less than those for SAT runs. Higher frequency of events simulated by assimilation runs matches the forecast. For most cases, SAT runs show better results after 12 to 24 hours of forecast time. This may indicate that the assimilated data may first affect the outer regions of the domain before it reaches the centre of the MD. This is consistent with results from Chou and Huang (2011). The statistical scores show that SAT runs have higher efficiency in simulating the observed rainfall than CNTL runs.

5. Conclusions

This study aims to understand the improvements in the model initial conditions achieved through the assimilation of satellite radiances and the consequent impact on the simulation of rainfall and other meteorological features associated with MDs. Eight MD cases that occurred during 2015-2018 are considered for this study.

To assess the impact of satellite radiance assimilation on initial conditions, the background field departure of BT (O-B) is compared with the analysis field departure of BT (O-A). The values of O-A are much less than the background field departure. RMSE and correlation coefficients calculated for model BT compared to observation show that SAT runs have higher correlation values and lower RMSE values. There is also considerable improvement in simulating vertical profiles of temperature and specific humidity, especially in layers between 500 hPa and 1000 hPa. Values of mean bias for vertical profiles showed a considerable reduction after assimilation. This suggests that the initial conditions of the model improved after the assimilation of satellite radiances. However, no improvement is seen in the biases of windspeeds of SAT runs compared to CNTL runs.

The track simulated by assimilation runs matches reasonably well with the IMD best track. SAT runs have slightly higher track error for initial forecast lengths of 0-9 hours, but as the forecast length increases, there is a considerable reduction in track error. SAT runs are also able to simulate the north-northwestward movement of MDs. The results indicate assimilation of radiances has a positive impact on track prediction. Improvements have been made in wind simulations mainly at upper tropospheric levels, after assimilation. While for lower-level winds, assimilation runs are reliable for a longer range forecast (>24h). For the entire forecast range, assimilation runs are more reliable and have lower RMSE values than CNTL runs at higher levels.

3DVAR simulated intensity and spatial distribution of precipitation are in better agreement with TRMM rainfall analysis as well as with IMD station observations. SAT runs were able to capture the location and intensity of maximum precipitation more accurately than CNTL runs. A statistically significant improvement in spatial mean rainfall prediction skill is seen in the number of stations clustered into different error bins, which shows that SAT runs reduced the number of stations in a higher rainfall error range (8-15 mm) to a lower error range (≤ 8 mm). Model forecast of precipitation is verified using various skill metrics like BIAS, CSI, and POD with different thresholds. For higher rainfall thresholds, 3DVAR runs have a higher value of CSI, higher BIAS, and higher POD. The statistical scores also stress that the precipitation forecast has improved in assimilation runs compared to CNTL runs.

This study thus shows that the assimilation of non-conventional data, like satellite radiance, leads to significant improvements in simulating features associated with MDs from a better representation of cold core to wind structure, track, and position and intensity of associated rainfall. Future direction in this area includes the incorporation of high-resolution land surface data assimilation. Land surface assimilation is important for MDs as they spend most of their time on land. So the characteristics of the land surface play an important role in the evolution of MDs. Also, studies with advanced assimilation techniques like 4DVAR, along with incorporating flow-dependent background error covariances, will help in validating the results.

Data availability

Satellite radiance data, TRMM 3B42, GPM L3 Final products, and ECMWF ERA5 data are available online from https://doi.org/10.5065/DWYZ-Q852, https://disc.gsfc.nasa.gov/, https://pmm.nasa.gov/data-access/downloads/gpm, and https://cds.climate.copernicus.eu/ datasets, respectively. The IMD provided station-wise precipitation estimates. The Best Track data are obtained from the IMD Regional Specialised Meteorological Centre (RSMC).

Funding

1. Space Application Centre (SAC), Ahmedabad (EOS-6/Oceansat-3 project)
2. Earth System Science Organization (ESSO), Ministry of Earth Sciences (MoES/16/14/2014-RDEAS), Government of India.

Acknowledgment

The authors acknowledge NIT Rourkela for providing the necessary infrastructure for research. They thank the Earth System Science Organization (ESSO), Ministry of Earth Sciences, Government of India, and the Space Application Centre (SAC), Ahmedabad, for providing the financial support to carry out this work.

Authors' contribution

Krishna K. Osuri: Conceptualizations, Methodology, Data Curation, Formal Analysis, Writing- Original Draft, Writing -Review; Editing, Funding acquisition.
Jharna Borah: Methodology, Formal Analysis, Visualization, Writing Review; Editing.
Koushik K.: Model runs, Formal Analysis, Data Curation, Visualization, Writing – Initial draft.
Y. Srinivas Nekkali: Methodology, Formal Analysis, Visualization, Writing Review; Editing.
Raghu Nadimpalli: Methodology, Formal Analysis, Writing Review; Editing.
Vijay Kumar Soni: Methodology, Formal Analysis, Writing Review; Editing.

Disclaimer: The contents and views presented in this research article/paper are the views of the authors and do not necessarily reflect the views of the organizations they belong to.

References

Ajayamohan, R.S., Merryfield, W.J. and Kharin, V.V., 2010, "Increasing trend of synoptic activity and its relationship with extreme rain events over central India", *J. Climate*, **23**, 4, 1004-1013. doi: https://doi.org/10.1175/2009JCLI2918.1.

Barker, D.M., W.Huang, Y. R. Guo, A. Bourgeois, and X. N. Xiao, 2004, "A three-dimensional variational data assimilation system for use with MM5: Implementation and initial results", *Mon. Wea. Rev*., **132**, 897–914. doi: https://doi.org/10.1175/1520-0493 (2004)132<0897:ATVDAS>2.0.CO;2.

Chou, C. B., and Huang, H. P., 2011, "The impact of assimilating atmospheric infrared sounder observation on the forecast of typhoon tracks. *Advances in Meteorology*, **1**, 803593. doi : https://doi.org/10.1155/2011/803593.

Courtier, P., E. Andersson, W. Heckley, J. Pailleux, D. Vasiljevic, M. Hamrud, A. Hollingsworth, F. Rabier and M. Fisher, 1998, "The ECMWF implementation of three-dimensional variational assimilation (3D-Var). Part 1: formulation", *Quart. J. Roy. Meteor. Soc.*, **124**, 1783-1807. doi : https://doi.org/10.1002/qj.49712455002.

Dee, D.P., 2005, "Bias and data assimilation, *Q. J. R. Meteorol. Soc.*, **131**, 613, 3323-3343. doi : https://doi.org/10.1256/qj.05.137.

Derber, J. C. and Wu W.S.,1998, "The use of TOVS cloud-cleared radiances in the NCEP SSI analysis system", *Monthly Weather Rev.*, **126**, 8, 2287-2299. doi : https://doi.org/10.1175/1520-0493(1998)126<2287:TUOTCC>2.0.CO;2.

Eyre, J. R., 1987, "On systematic errors in satellite sounding products and their climatological mean values. Quarterly Journal of the Royal Meteorological Society, **113**, 475, 279-292. doi : https://doi.org/10.1002/qj.49711347516.

Gadgil Sulochana, and Sidhartha Gadgil, 2006, "The Indian Monsoon, GDP and Agriculture, Econ. Pol. Weekly, XLI, 4887-4895.

Godbole, R. V., 1977, "The composite structure of the monsoon depression. Tellus, **29**, 1, 25-40. doi : https://doi.org/10.3402/tellusa.v29i1.11327.

Hersbach, H., Bell, B., Berrisford, P., Hirahara, S., Horányi, A., Muñoz-Sabater, J., ... & Thépaut, J. N., 2020, "The ERA5 global reanalysis", *Quarterly journal of the royal meteorological society*, **146**, 730, 1999-2049. doi : https://doi.org/10.1002/qj.3803.

Huffman, G. J., Bolvin, D. T., Braithwaite, D., Hsu, K., Joyce, R., and Xie, P., 2014, "Integrated multi-satellite retrievals for GPM (IMERG)", *Precipitation Measurement Missions Technical documentation*.

Hurley, J.V. and Boos ,W.R., 2015, "A global climatology of monsoon low pressure systems", *Q J R Meteorol Soc* **141**, 1049-1064. doi : https://doi.org/10.1002/qj.2447.

Karbou, F., Gérard, É., and Rabier, F., 2006, "Microwave land emissivity and skin temperature for AMSU-A and-B assimilation over land", *Quarterly Journal of the Royal Meteorological Society: A journal of the atmospheric sciences, applied meteorology and physical oceanography*, **132**, 620, 2333-2355. doi : https://doi.org/10.1256/qj.05.216.

Krishnamurty, T. N. and Bhalme, H. N., 1976, "Oscillations of a monsoon system Pt. I Observational aspects", *Journal of Atmospheric Sciences*, **33**, 1937-1954.

Kutty, G., and Wang, X., 2015, "A comparison of the impacts of radiosonde and AMSU radiance observations in GSI based 3DEnsVar and 3DVar data assimilation systems for NCEP GFS. *Advances in Meteorology*, **1**, 280546. doi : https://doi.org/10.1155/2015/280546.

Mooley, D.A., Shukla J., 1989, "Main features of the westward-moving low pressure systems which form over the Indian region during the summer monsoon season and their relation to the monsoon rainfall", *Mausam*, **40**, 2, 137-152. doi : https://doi.org/10.54302/mausam.v40i2.2041.

Osuri, K. K., Mohanty, U.C., Routray, A. and Niyogi, D., 2015, "Improved prediction of Bay of Bengal tropical cyclones through assimilation of Doppler weather radar observations", *Monthly Weather Review*, **143**, 11, 4533-4560. doi : https://doi.org/10.1175/MWR-D-13-00381.1.

Parrish, D. F., and J. C. Derber, 1992, "The National Meteorological Center's spectral statistical-interpolation analysis system", *Mon. Wea. Rev*., **120**, 1747-1763. doi : https://doi.org/10.1175/1520-0493(1992)120<1747:TNMCSS>2.0.CO;2.

Rakesh, V., Singh, R. and Joshi, P. C., 2010, "Impact of four dimensional assimilation of satellite data on long-range simulations over the Indian region during monsoon 2006. Advances in space research, **46**, 7, 895-908. doi : https://doi.org/10.1016/j.asr.2010.05.013.

Routray, A., Mohanty, U.C., Osuri, K. K. and Prasad, S. K., 2013, Improvement of monsoon depressions forecast with assimilation of Indian DWR data using WRF-3DVAR analysis system. *Pure and Applied Geophysics*, *170*, 12, 2329-2350. doi : https://doi.org/10.1007/s00024-013-0648-z.

Routray, A., Kar, S. C., Mali, P., and Sowjanya, K., 2014, "Simulation of monsoon depressions using WRF-VAR: impact of different background error statistics and lateral boundary conditions", *Monthly Weather Review*, **142**, 10, 3586-3613. doi : https://doi.org/10.1175/MWR-D-13-00285.1.

Routray, A., Mohanty, U. C., Osuri, K. K., Kar, S. C. and Niyogi, D., 2016, "Impact of satellite radiance data on simulations of Bay of Bengal tropical cyclones using the WRF-3DVAR modeling system", *IEEE Transactions on Geoscience and Remote Sensing*, **54**, 4, 2285-2303. doi : https://doi.org/10.1109/TGRS.2015. 2498971.

Sikka, D.R., 1977, "Some aspects of the life history, structure and movement of monsoon depressions. Pure Appl Geophys 115:1501-1529. doi: https://doi.org/10.1007/978-3-0348-5759-8_21

Skamarock, W. C., J. B. Klemp, J. Dudhia, D. O. Gill, D. M. Barker, W. Wang, and J. G. Powers, 2005, "A description of the advanced research WRF version 2. NCAR Tech. Note NCAR/TN-4681STR, p88. DOI: https://doi.org/10.5065/D68S4MVH.

Wilks, D. S., 2011, Statistical methods in the atmospheric sciences (3rd ed.). Oxford; Waltham, MA: Academic Press.

Yang, F., 2014, "Historical performances of global NWP models", NCEP/EMC/Global Climate and Weather Modeling Branch.

Zapotocny, T. H., Jung, J. A., Le Marshall, J. F., and Treadon, R. E. 2008, "A two-season impact study of four satellite data types and rawinsonde data in the NCEP Global Data Assimilation System", *Weather and Forecasting*, **23**, 1, 80-100. doi : https://doi.org/10.1175/2007WAF2007010.1